

## Nonlinear Excitations in Dust-Ion Acoustic Waves and the Formation of Rogue Waves in Stable Parametric Region in a 3-Component Degenerate Plasma

P. Samanta<sup>1</sup>, A. De<sup>1</sup>, S. Dey<sup>2</sup>, D. Maity<sup>2</sup>, A. Ghosh<sup>3</sup> and S. Chandra<sup>4,\*</sup>

<sup>1</sup> Physics Department, Scottish Church College, Kolkata 700006, India

<sup>2</sup> Department of Physics, Visva-Bharati University, Santiniketan, Bolpur, West Bengal-731235, India

<sup>3</sup> Department of Physics, Bethune College University of Calcutta, Kolkata, West Bengal-700006, India

<sup>4</sup> Department of Physics, Government General Degree College at Kushmandi, India, 733121.

\* Institute of Natural Sciences and Applied Technology, Kolkata, India, 700032.

E-mail: swarniv147@gmail.com (corresponding author)

In this work, nonlinear propagation of dust-ion-acoustic waves in 3 component plasma with electrons and ions being degenerate in ultra-relativistic limit is studied. The Korteweg de—Vries Burgers (KdV-B) equation is derived by the standard reductive perturbation method. It is found to admit solutions for electrostatic solitary and shock profiles, whose basic features have been analysed numerically. The dynamics of the system is studied in perturbed and unperturbed system in detail. We also developed Nonlinear Schrodinger equation and from this we obtained the Rogue wave then analysed the various properties of it. We also examined a possible way to generate a Rogue wave and the stability of that wave in some particular condition with various parameters. We obtained a critical condition of existence of a stable wave.

### 1. Introduction

Compact astrophysical objects like white dwarfs and neutron stars keep themselves from collapsing under the immense gravitational force at the core by quantum degeneracy pressure. At these extreme conditions, quantum effects start dominating and the star is no more supported by thermal energy. Equation of state of such a system is provided by S. Chandrasekhar. At ultra-relativistic limits, the equation of state is,  $p = (1/8)(3/\pi)^{1/3} hcn^{4/3}$ . Due to the dominant quantum effects, we made a quantum hydrodynamic model (QHD) of the system. At such high densities, the de-Broglie wavelength of the electrons overlaps causing Bohm potential, exchange and correlation energy to have significant effects on the propagation of electrostatic waves. Similar QHD models were studied by Zobaer et al [1].

We have considered relativistic velocities for all components and ultra-relativistic degeneracy in only ions and electrons. “Rogue waves” (RWs) have typically very large amplitude and can generated more frequently than expected. Generally, Rouge waves have amplitude more than twice or thrice of a significant wave amplitude, will

appear suddenly and disappeared without living a trace [2], [3] but we can localize. Korteweg–de Vries equation Burgers (KdV-B), non-linear Schrodinger equation (NLSE) has been developed to analyse the results of such non-linear systems like space plasma and planetary plasmas. The dynamical properties of a non-linear Rogue waves can be analysed by NLSE.

### 2. Governing Equations

Continuity equation for dust, ions and electrons is given as,

$$\frac{\partial n_j}{\partial t} + \frac{\partial}{\partial x}(n_j u_j) = 0 \quad (1)$$

where  $j$  is  $d, i, e$  for dust, ions and electrons respectively and  $n_j, u_j$  are the number density and velocity of the respective species. Equation of motion for dust, ions and electrons is respectively given as,

$$\left( \frac{\partial}{\partial t} + u_d \frac{\partial}{\partial x} \right) u_d \gamma_d = \frac{Q_d}{m_d} \frac{\partial \phi}{\partial x} + \frac{1}{m_d} \eta_d \frac{\partial^2 u_d}{\partial x^2} \quad (2)$$

$$\left( \frac{\partial}{\partial t} + u_i \frac{\partial}{\partial x} \right) u_i \gamma_i = \frac{1}{m_i} \left( Q_i \frac{\partial \phi}{\partial x} - \frac{1}{n_i} \frac{\partial p_i}{\partial x} \right) + \frac{1}{m_i} \eta_i \frac{\partial^2 u_i}{\partial x^2} \quad (3)$$

$$\left(\frac{\partial}{\partial t} + u_e \frac{\partial}{\partial x}\right) u_e \gamma_e = \frac{1}{m_e} \left( Q_e \frac{\partial \phi}{\partial x} - \frac{1}{n_e} \frac{\partial p_e}{\partial x} \right) + \frac{\hbar^2}{2m_e^2 \gamma_e} \frac{\partial}{\partial x} \left( \frac{1}{\sqrt{n_e}} \frac{\partial^2 \sqrt{n_e}}{\partial x^2} \right) + \frac{e}{m_e} \frac{\partial (U_{xc,e})}{\partial x} \quad (4)$$

$$\frac{\partial^2 \phi}{\partial x^2} = 4\pi e (n_e + Z_d n_d - Z_i n_i) \quad (5)$$

Where  $\phi$  is the electrostatic potential,  $Q_e = e$ ,  $Q_d = Z_d$ ,  $Q_i = -Z_i e$ ,  $Z_j$  is the number of effective charges of each species (for ions it is the average ionisation, for dust it is average number of electrons accumulated on it),  $m_j$  is the mass of each species,  $\eta_j$  is the dissipation coefficient of dust and ions. Relativistic momentum of the species gives the Lorentz factor  $\gamma_j = \frac{1}{\sqrt{1 - u_j^2 / c^2}}$

for the respective species. The ultra-relativistic pressure is given by the  $p_j = \frac{1}{8} \left( \frac{3}{\pi} \right)^{1/3} h c n_j^{4/3}$ . As

mentioned, the Bohm potential and exchange correlation energy becomes important for consideration for electrons with the longest de-Broglie wavelengths of all other species. They are given by the second and third terms on the right-hand side of equation.  $\hbar$  is the reduced Planck's Constant.

$U_{xc,e} = \Gamma_e^{exc} + \Gamma_e^{cor}$  represents the sum of exchange and correlation potentials (which doesn't involve any actual force field and is completely a quantum artifact).

$$\Gamma_e^{exc} = -0.985 \frac{e^2}{\varepsilon} n_e^{1/3}$$

$$\Gamma_e^{cor} = 0.03349 \frac{e^2}{\varepsilon a_b} \left( 1 + \ln \left| 1 + 18.376 a_b n_e^{1/3} \right| \right)$$

$a_b = \varepsilon \hbar^2 / e^2 m_e$ ,  $\varepsilon$ , is the relative permeability of the plasma medium. Simplifying we obtain,

$$U_{xc,e} = -1.6 \frac{e^2}{\varepsilon} n_e^{1/3} + 5.65 \frac{\hbar^2}{m_e} n_e^{2/3}$$

### 3. Normalized Equations

Normalised continuity equations for dust, ions and electrons are given as,

$$\frac{\partial n_j}{\partial t} + \frac{\partial}{\partial x} (n_j u_j) = 0 \quad (6)$$

Equation of motion for dust, ions and electrons is respectively given as,

$$\left(\frac{\partial}{\partial t} + u_d \frac{\partial}{\partial x}\right) u_d \gamma_d = \mu_d z_d \frac{\partial \phi}{\partial x} + \eta_d \frac{\partial^2 u_d}{\partial x^2} \quad (7)$$

$$\left(\frac{\partial}{\partial t} + u_i \frac{\partial}{\partial x}\right) u_i \gamma_i = -\mu_i z_i \frac{\partial \phi}{\partial x} + \eta_i \frac{\partial^2 u_i}{\partial x^2} - \mu_i \sigma_i n_e^{-\frac{2}{3}} \frac{\partial n_e}{\partial x} \quad (8)$$

$$\left(\frac{\partial}{\partial t} + u_e \frac{\partial}{\partial x}\right) u_e \gamma_e = \lambda_{2,e} n_e^{-\frac{1}{3}} \frac{\partial n_e}{\partial x} - \lambda_{1,e} n_e^{-\frac{2}{3}} \frac{\partial n_e}{\partial x} - \frac{\partial \phi}{\partial x} - \sigma_e n_e^{-\frac{2}{3}} \frac{\partial n_e}{\partial x} + \frac{H^2}{2\gamma_e} \frac{\partial}{\partial x} \left[ \frac{1}{\sqrt{n_e}} \frac{\partial^2 \sqrt{n_e}}{\partial x^2} \right] \quad (9)$$

$$\frac{\partial^2 \phi}{\partial x^2} = n_e + n_d \delta_d - n_i \delta_i \quad (10)$$

Here,

$$\sigma_j = \frac{A n_{j0}^{1/3}}{m_e V_{Fe}}, \quad A = \frac{1}{6} \left( \frac{3}{\pi} \right)^{1/3} h c, \quad H = \frac{\hbar \omega_e}{2 K_B T_{Fe}} .$$

$$\lambda_{2,e} = \frac{3.77 \hbar^2 n_{e0}^{2/3}}{m_e E_{Fe}}, \quad \lambda_{1,e} = \frac{1.6 e^2 n_{e0}^{1/3}}{3 \varepsilon E_{Fe}}$$

The dimensionless scaling factors used are

$$\mu_j = \frac{m_e}{m_j} \text{ and } \delta_j = \frac{z_j n_{j0}}{n_{e0}} .$$

### 4. Linear Dispersion Relation

We assume the field parameters to vary with the form,  $\phi = \phi_0 e^{i(kx - \omega t)}$ , where  $k$  and  $\omega$  are the normalized wave number and frequency respectively. For the linearization we used the following expansion,

$$\begin{bmatrix} n_j \\ u_j \\ \phi \end{bmatrix} = \begin{bmatrix} 1 \\ u_{j0} \\ \phi_0 \end{bmatrix} + \varepsilon \begin{bmatrix} n_j^{(1)} \\ u_j^{(1)} \\ \phi^{(1)} \end{bmatrix} + \varepsilon^2 \begin{bmatrix} n_j^{(2)} \\ u_j^{(2)} \\ \phi^{(2)} \end{bmatrix} + \dots \quad (11)$$

where  $j$  is  $d, i, e$  for dust, ions and electrons respectively and  $n_j$ ,  $u_j$  are the normalised number density and normalised velocity of the respective species. Just using the first order perturbations we obtain the following linear dispersion relation,

$$k^2 = \frac{A_d}{f_d^2 \left( g_d + \frac{ik\eta_d}{f_d} \right)} + \frac{A_i}{f_i^2 \left( g_i + \frac{i\eta_i k}{f_i} \right)} - C_i + \frac{1}{f_e^2 g_e - \frac{H^2 k^2 \gamma_{e0}}{4} - C_e} \quad (12)$$

where  $f_j = u_{j0} - \frac{\omega}{k}$ ,  $\gamma_{j0} = \sqrt{1 - \frac{u_{j0}^2}{c^2}}$ ,  $g_j = \gamma_{j0} - \left( \frac{u_{j0}}{c} \right)^2$ ,  $A_j = \mu_j \delta_j z_j$ , (in case of electrons this constant is 1), where  $j$  refers to dust, ions and electrons.  $C_e = 1 + \lambda_{1e} - \lambda_{2e}$ ,  $C_i = \mu_i \sigma_i$ .

As we have considered a dissipating system,  $k$  is complex. The tedious substitutions and simplifications were carried out using the sympy module in python. In DIAW's the frequency is well below plasma frequency causing the normalised frequency  $\omega$  to be well below 1, hence neglecting higher orders of  $\omega$  is a good approximation. For white dwarfs it can be shown that higher powers of  $k \approx 0$  is a good approximation for any practical wavelengths and we are working with acoustic modes. The dispersion relation so obtained has been plotted in the figure below.

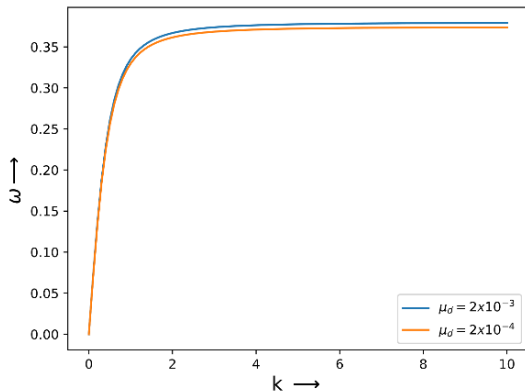


**Fig.1:**  $\omega$  varies linearly with  $k$  at long wavelength range and the group velocity is very high.

## 5. Derivation of KdV-B equation

We used transformations  $\xi = \varepsilon^{1/2}(x - V_0 t)$ ,  $\tau = \varepsilon^{3/2} t$  and  $\eta_j = \varepsilon^{1/2} \eta_{j0}$  in the above equations. Where,  $\varepsilon$  is the smallness parameter measuring the weakness of the dispersion  $V_0$  is the phase velocity. The  $\varepsilon^{3/2}$  terms in continuity and momentum equations give the following linear relations between the first order perturbations in the field parameters,

$$u_j^{(1)} = (V_0 - u_{j0}) n_j^{(1)} \quad (13)$$

$$\phi^{(1)} = N_j u_j^{(1)}$$

(14)

Where,  $j = d, i, e$  for dust, ions and electrons respectively. Here,

$$N_d = \frac{-V_0 \frac{u_{d0}^2}{c^2} - (V_0 - u_{d0}) \gamma_{d0} + \frac{u_{d0}^3}{c^2}}{\mu_d z_d}$$

$$N_i = \frac{-V_0 \frac{u_{i0}^2}{c^2} - (V_0 - u_{i0}) \gamma_{i0} + \frac{u_{i0}^3}{c^2} - \frac{2\sigma_i \mu_i}{3(V_0 - u_{i0})}}{-\mu_i z_i}$$

$$N_e = -V_0 \frac{u_{e0}^2}{c^2} - (V_0 - u_{e0}) \gamma_{e0} + \frac{u_{e0}^3}{c^2} - \frac{2\sigma_e + 2\lambda_{1e} - \lambda_{2e}}{3(V_0 - u_{e0})}$$

From the  $\varepsilon^2$  terms and then differentiating once with respect to  $\xi$ ,

$$\frac{\partial^3 \phi^{(1)}}{\partial \xi^3} = \frac{\partial n_e^{(2)}}{\partial \xi} + \delta_d \frac{\partial n_d^{(2)}}{\partial \xi} + \delta_i \frac{\partial n_i^{(2)}}{\partial \xi}$$

(15)

From the  $\varepsilon^3$  terms we obtain,

$$\frac{\partial^2 \phi^{(2)}}{\partial \xi^2} = n_e^{(3)} + \delta_d n_d^{(3)} + \delta_i n_i^{(3)}$$

Third order perturbations at  $\xi \rightarrow$  large, is small enough to be neglected in our investigation. After integration with respect to  $\xi$  leads to,  $\frac{\partial \phi^{(2)}}{\partial \xi} \approx 0$ . From the  $\varepsilon^{5/2}$  terms of the

continuity and momentum equations, we get the

non-linear equations. Performing some simple algebraic substitutions and using the above equation we obtain the KdV-B equations as follows,

$$\frac{\partial \phi^{(1)}}{\partial \tau} + A \frac{\partial^3 \phi^{(1)}}{\partial \xi^3} + B \phi^{(1)} \frac{\partial \phi^{(1)}}{\partial \xi} + C \frac{\partial^2 \phi^{(1)}}{\partial \xi^2} = 0$$

Using the transformations  $\chi = \xi - V_0$ , we obtain the KdV-B equation in the frame of the plasma wave as follows,

$$-V_0 \frac{\partial \phi^{(1)}}{\partial \chi} + A \frac{\partial^3 \phi^{(1)}}{\partial \chi^3} + B \phi^{(1)} \frac{\partial \phi^{(1)}}{\partial \chi} + C \frac{\partial^2 \phi^{(1)}}{\partial \chi^2} = 0$$

(16)

The well-known series solution to this by Wazwaz is,

$$\psi = \frac{12B}{A} [1 - \tanh^2(\chi)] - \frac{36C}{15A} [\tanh^2 \chi] \quad (17)$$

where  $\psi$  is equal to  $\phi^{(1)}$ .

This is a shock profile as shown below in the plot of  $\psi$  vs  $\chi$  for different values of Mach's number.

Where,

$$D = -\left( \frac{\delta_d p_1^d}{p_2^d} + \frac{\delta_i p_1^i}{p_2^i} + \frac{p_1^e}{p_2^e} \right), A = \frac{\left( \frac{p_4^e}{p_2^e} - 1 \right)}{D}$$

$$B = \frac{-\left( \frac{\delta_i p_3^i}{p_2^i} + \frac{p_3^e}{p_2^e} - \frac{\delta_d p_3^d}{p_2^d} \right)}{D}, C = \frac{\left( \frac{\delta_i p_4^i}{p_2^i} + \frac{\delta_d p_4^d}{p_2^d} \right)}{D}$$

$$p_1^j = \frac{1}{N_j} \left( S_1^j - \frac{S_2^j}{V_0 - u_{j0}} \right), p_3^j = \frac{1}{N_j^2} \left( S_3^j - \frac{2S_2^j}{V_0 - u_{j0}} \right),$$

$$p_2^e = -\left( \frac{2}{3} (\sigma_e + \lambda_{1e}) - \frac{\lambda_{2e}}{3} \right) - S_2^e (-V_0 + u_{e0}),$$

$$p_4^e = \frac{S_4^e}{N_e}, p_2^d = S_2^d (V_0 - u_{d0}), p_4^d = \frac{\eta_d}{N_d},$$

$$p_2^i = -2 \frac{\mu_i \sigma_i}{3} - 2S_2^i (V_0 - u_{i0}),$$

$$p_4^i = \frac{\eta_{i0}}{N_i}, S_1^j = \gamma_{j0} + \left( \frac{u_{j0}}{c} \right)^2, S_2^j = \frac{u_{j0}}{c^2} (u_{j0}^2 - u_{j0} V_0) +$$

$$\gamma_{j0} (u_{j0} - V_0)$$

$$S_3^e = \alpha^e - \frac{\lambda_{2e} - 4(\sigma_e + \lambda_{1e})}{9(V_0 - u_{e0})^2}, S_4^e = \frac{H^2}{4\gamma_{e0}(V_0 - u_{e0})}$$

$$S_3^i = \alpha^i + \frac{4\sigma_i \mu_i}{9} (V_0 - u_{i0})^2, S_3^d = \alpha^d,$$

$$\alpha^j = \gamma_{j0} + \left( \frac{u_{j0}}{c} \right)^2 + 3 \frac{u_{j0}}{c^2} (u_{j0} - V_0)$$

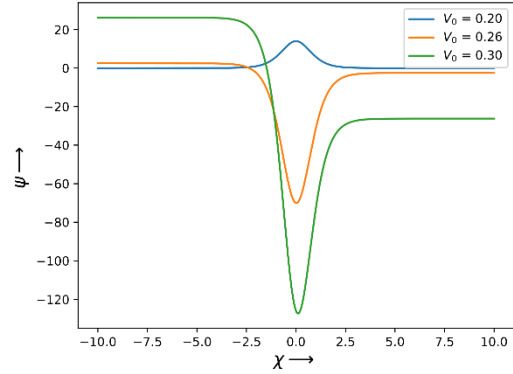


**Fig.2:** Shock profile for parameter values,  $H = 1, \delta_i = 1.5, \delta_d = 0.5$ .

At  $V_0 = 0.20$  a compressive soliton can be seen but around  $V_0 = 0.21$  it becomes rarefactive soliton and also develops into a shock wave with further higher values of Mach number.

## 6. Calculation of NLSE and 'Peregrine' soliton of Rogue wave for the system

A method to study Rogue waves by mathematics is based on examining Nonlinear Schrodinger equation (NLSE). From the reductive perturbative technique, we approximated dispersion property and nonlinear property to the lowest order perturbation. We define a 'Peregrine' solution using the lowest order perturbation. A higher accurate model is been developed by taking account higher-order approximations. We developed the lowest order perturbed solution of NLSE by taking the linear potential which is time-dependent.

To transform KdV B to NLSE we use Fourier expansion method of the corresponding field as:

$$\psi = \sum_{q=1}^{\infty} \mathcal{E}^q \sum_{s=-q}^q \psi_s e^{is\Phi}, \psi_s = \sum_{s=0}^{\infty} \mathcal{E}^s \bar{\psi}_s^{(s)} \quad (18)$$

$\phi_0$  and  $\psi_s$  are slowly varying quantity with respect to time and space.

Expanding the quantity  $\psi$  we get a form:

$$\psi = (\varepsilon \bar{\psi}_0 + \varepsilon \bar{\psi}_0^*) + (\varepsilon \bar{\psi}_0 e^{i\Phi} + \varepsilon \bar{\psi}_1^* e^{-i\Phi}) + (\varepsilon^2 \bar{\psi}_2 e^{2i\Phi} + \varepsilon^2 \bar{\psi}_2^* e^{-2i\Phi}) + \dots$$

Defining new stretching variables (where 'c' is the group velocity),

$$\rho = \varepsilon [\xi - c_g \tau] \quad \text{and} \quad \theta = \varepsilon^2 \quad (19)$$

By changing all variables in terms of  $\rho$  and  $\theta$  as well using perturbation we get,

$$\frac{\partial}{\partial \tau} = -is\omega - \varepsilon c_g \frac{\partial}{\partial \rho} + \varepsilon^2 \frac{\partial}{\partial \theta}$$

$$\frac{\partial}{\partial \xi} = isk + \varepsilon \frac{\partial}{\partial \rho}$$

Equating the coefficients of  $e^{i\Phi}$  including  $\varepsilon$  from perturbation expansion we will get,

$$\omega = -Ak^3 + ick^2 \quad (20a)$$

$$c = V_g = \frac{\partial \omega}{\partial k} = -3Ak^2 + 2ick \quad (20b)$$

In similar way equating the coefficients of  $e^{2i\Phi}$  with  $\varepsilon^2$  from perturbation relation we get,

$$\bar{\psi}_2^{(1)} = \frac{B}{6Ak^2} \bar{\psi}_1^{2(1)} \quad (20c)$$

Equating both for the first harmonics terms,

$$i \frac{\partial \bar{\psi}_1^{(1)}}{\partial \theta} + \frac{P}{2} \frac{\partial^2 \bar{\psi}_1^{(1)}}{\partial \rho^2} + Q \bar{\psi}_1^{2(1)} \bar{\psi}_1^{*(1)} = 0 \quad (21)$$

considering that  $\bar{\psi}_1^{(1)} \equiv \Psi$ ,

$$i \frac{\partial \Psi}{\partial \theta} + \frac{P}{2} \frac{\partial^2 \Psi}{\partial \rho^2} + Q \Psi^2 \Psi^* = 0 \quad (22)$$

Where, we get  $P = -6Ak - 2C$  and  $Q = -\frac{B^2}{6kA}$ .

$PQ < 0$  as  $C < 0$  suggests that the wave will be in stable region. Approaching to a rational a *Peregrine*

soliton which gives for first order variation:

$$\Psi = \sqrt{\frac{P}{Q}} \left[ \frac{4(1+2iP\theta)}{(1+4\rho^2+4P^2\theta^2)} - 1 \right] e^{iP\rho} \quad (23)$$

$$|\Psi| = \left| \sqrt{\frac{P}{Q}} \right| \times \sqrt{\left( \frac{4}{(1+4\rho^2+4P^2\theta^2)} - 1 \right)^2 + \frac{64P^2\theta^2}{(1+4\rho^2+4P^2\theta^2)^2}} \quad (24)$$

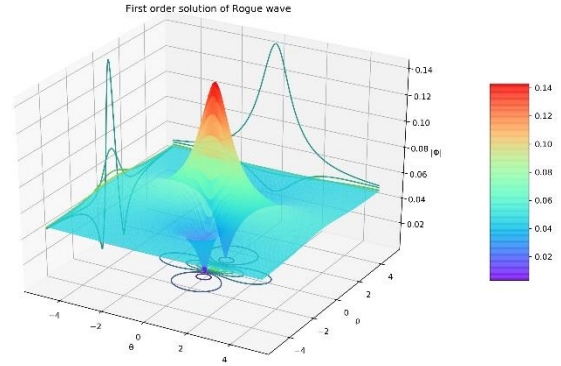


**Fig.3:** 'Peregrine' soliton of Rogue wave plotted against  $\theta$  and  $\rho$

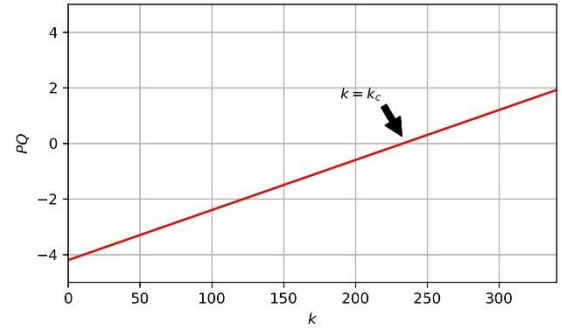


**Fig.4:**  $PQ$  plotted against  $k$  to find the stability.

we see it is clear that  $P < 0$  and  $Q > 0$ , for at least must be  $0 < k < 2$ .

$PQ = \frac{(6Ak + 2C)B^2}{3Ak} < 0$  so plotting  $PQ$  over

different quantities like Mach Number ( $M$ ), streaming velocity ( $v_0$ ) we determined the critical condition  $k = k_c$  for stability of Rogue wave (Fig. 4).

## 7. Dynamics of the system

### 7.1 Unperturbed Dynamics

After deriving the existence of shock profiles this paper would determine how this shock propagates and evolves, how it responds to small perturbations, its stability and how the system responds to very small changes in initial conditions that is its chaotic behaviour. Similar elaborate studies on were done on Thomas-fermi plasma [4] and electron-acoustic super non-linear waves [5]. First, we would give a brief account of the unperturbed dynamics of the system. Integrating Equation (16) once with respect to  $\chi$ ,

$$A \frac{\partial^2 \psi}{\partial \chi^2} + \left( -V_0 \psi + B \frac{\psi^2}{2} \right) \frac{\partial \psi}{\partial \chi} + C \frac{\partial \psi}{\partial \chi} = 0 \quad (25)$$

Integrating again we obtain,

$$A \frac{\partial \psi}{\partial \chi} + \left( -V_0 \frac{\psi^2}{2} + B \frac{\psi^3}{6} \right) \psi + C \psi = 0 \quad (26)$$

Taking  $\zeta = \frac{\partial \psi}{\partial \chi}$ , equation (25) becomes,

$$A \zeta' = -C \zeta + \left( V_0 \psi - B \frac{\psi^2}{2} \right) \quad (27)$$

Where  $\zeta' = \frac{\partial^2 \psi}{\partial \chi^2}$ . Solving this numerically and

plotting  $\zeta$  vs  $\psi$  we obtain the following.

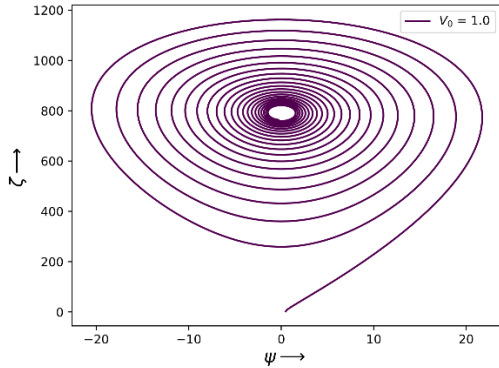


**Fig.5:** Phase trajectory of the system with initial conditions  $\zeta_0 = 2.5, \psi_0 = 0.5$  and the attractor is approximately at  $(\zeta_0, \psi_0) = (800.0, 0.0)$ .

The shock profile shown in figure (2) is the structure of the wave. In this section we are analysing how it propagates through space and evolves in time. But it is necessary a priori to understand that the figure (5) and the differential

equation in (27) doesn't denote the trajectory in physical space. It is a phase trajectory that is the variation of the quasi velocity with quasi position as the quasi time evolves.

It is evident from figure (5) that the system orbits around some point. Then as quasi-time evolves, the orbit decays and the system approach the point. After we have allowed a large amount of time to the system to evolve one evidently notices by looking close into figure (5) that it becomes apparently stable in an orbit very close to the point. This point is called attractor.

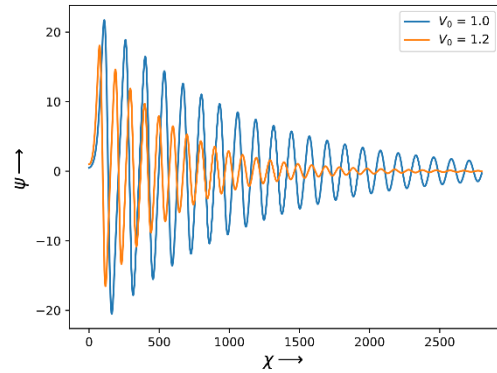


**Fig.6:** This represents the periodic DIAWs. The periodic variation with quasi-time is shown here.

### 7.2 Perturbed Dynamics

So far, we dealt with a system which has no external source of disturbance. Now we shall in detail investigate the evolution of a small periodic external driving force on the system. We choose the periodic force to be  $f_0 \cos(\omega \chi)$ . We get a modified equation (27) as,

$$A \zeta' = -C \zeta + \left( V_0 \psi - B \frac{\psi^2}{2} \right) + f_0 \cos(\omega \chi) \quad (28)$$

We employed the numerical technique and obtained the phase trajectory of the perturbed dynamical system. Here we have provided different initial conditions, that is 2 different values of  $\zeta(\chi = 0), \psi(\chi = 0)$ .

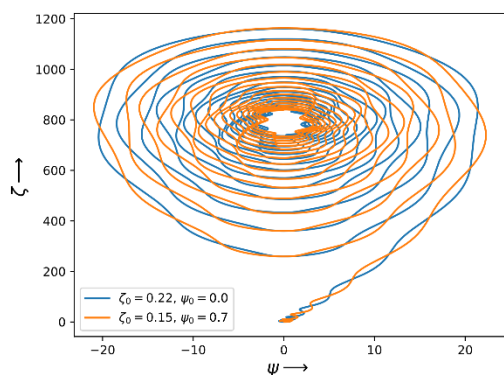


**Fig.7:** The amplitude and frequency of the driving force is given as,  $f_0 = 0.2$  and  $\omega = 0.3$ .

Notice the difference in trajectories in figure (7) owing just to the very small difference in initial conditions. The trajectories represented with blue and orange have initial conditions  $(\zeta_0, \psi_0) = (0.22, 0.0)$  and  $(0.15, 0.7)$  respectively. By just looking at the early evolution of the system it may be tempting to declare it as a largely chaotic system but that is not the case. The reason is that at the later part of the evolution, both of the trajectories eventually approach a stable orbit around the same attractor. It hints at a single stability of the system. In our future work we would work upon Lyapunov exponents in an attempt to find whether other hidden attractors exist.

## 8. Conclusion

We have obtained a shock profile for a relativistic degenerate dense dusty plasma which showed its high response towards varying Mach number. The stability of the system was studied in detail. Assuming periodic driving force it was shown that the system hints at a single stability. This study can be applied to study of shock waves in the plasma environment of compact astrophysical objects such as white dwarfs. The shock waves which is supposed to transports large part of the energy in these environments seems to be quite stable and not much chaotic.

We studied the first-order solution for Rogue wave and plotted it against  $\theta$  and  $\rho$  also projected along three planes. By adopting values of  $P$  and  $Q$  we obtained the Rouge wave. The spatial part as well

as temporal behaviour of Rogue wave has been discussed here. Peak of the wave determines how intense the potential is. For a particular  $\rho$  value there is a critical value of  $\theta (= \theta_c)$  value also for a particular  $\theta$  we can get a critical value of  $\rho (= \rho_c)$ . Using the perturbing technique, we have shown the wave envelope solutions as shown in Fig. 3.

So far, we have studied the stability of this wave generated by the system. For the critical case as for  $P = 0$ . Where we get,

$$k = k_c = \left| \frac{C}{3A} \right|$$

It is clear that if we set  $A \rightarrow 0$  in Fig. 4 then  $PQ$  becomes goes to negative value so then there will be no instability as well as the equation drops to KdV-NLSE. So, for this case wave is stable for that particular reason Rogue wave cannot be generated further. Also, the value of  $k$  is too large for which we have got a critical condition in other way we have got critical condition when  $\omega$  saturated for large  $k$  values.

## Acknowledgements

The authors would like to thank the reviewers for their valuable inputs towards upgrading the paper. Authors would like to thank the Institute of Natural Sciences and Applied Technology, the Physics departments of Jadavpur University and Government General Degree College at Kushmandi for providing facilities to carry this work. We also thank our family and friends for their support, patience and encouragement.

## References

- [1] M. S. Zobaer, Roy.N and A.A. Mamun, *Astrophysics and Space Science*, **72(7)**, 343, (2013).
- [2] N. Akhmediev, J.M. Soto-Crespo and A. Ankiewicz, *Physics Letters A*, **373(25)**, 2137, (2009).
- [3] N. Akhmediev, A. Ankiewicz and M. Taki, *Physics Letters A*, **373(6)**, 675, (2009).
- [4] A. Saha, S. Sarkar and S. Banerjee, *The European Physical Journal Special Topics*, **229** (2020).
- [5] A. Abdikian, J. Tamang and A. Saha, *Communications in Theoretical Physics*, **72(7)**, 075502, (2020).

The African Review of Physics (2020) **15**  
Special Issue on Plasma Physics: 002

- [6] S. Chandra, S. N. Paul, and B. Ghosh, *Astrophysics and Space Science*, **343(1)**, 213, (2013).
- [7] J. Goswami, S. Chandra, B. Ghosh. *Astrophysics and Space Science*, **364(4)**, 65, (2019).
- [8] J. Sarkar, S. Chandra, J. Goswami, B. Ghosh, *Contributions to Plasma Physics*, **60(7)**, e201900202, (2020)
- [9] S. Chandra, J. Goswami, J. Sarkar, C. Das, *Journal of Korean Physical Society*, **76**, 469 (2020)

Received: 24<sup>th</sup> September, 2020

Accepted (revised version): 20<sup>th</sup> December, 2020